Available online at www.sciencedirect.com
SCIENCE DIRECT®
Geochimica et Cosmochimica Acta 70 (2006) 3986–3995
Geochimica
www.elsevier.com/locate/gca

# Germanium isotope measurements of high-temperature geothermal fluids using double-spike hydride generation MC-ICP-MS

Christopher Siebert [a,*], Andy Ross [b], James McManus [b]

[a] Department of Geological Sciences, Arizona State University, Box 871404, Tempe, AZ 85287-1404, USA
[b] Oregon State University, College of Oceanic and Atmospheric Sciences, 101 SW 26th Street, COAS Admin. Bldg. Corvallis, OR 97330-5503, USA

Received 14 September 2005; accepted in revised form 5 June 2006

**Abstract**

We present a double-spike isotope dilution MC-ICP-MS technique for the determination of germanium (Ge) isotope fractionation. Using this technique we determined Ge isotope compositions of geothermal spring fluids, a Columbia River Basalt sample, and an in-house diatom standard. Our technique uses a $^{73}Ge/^{70}Ge$ double spike in combination with hydride generation for Ge extraction from the sample matrix. Fractionation is determined on the $^{74}Ge/^{72}Ge$ mass ratio. The double spike allows us to effectively correct analytical isotope fractionation. Our external standard reproducibility is 0.4‰ (2 SD) over the course of several months. The minimum quantity of Ge needed for isotope analysis is approximately 2 ng. Consistent with previous work on geothermal fluids, Ge in the geothermal spring samples presented here is enriched over Si as compared to low temperature weathering signatures. This observation is typically interpreted as Ge exclusion during silicate mineral precipitation (e.g., quartz). Our isotope results indicate that the analyzed high temperature fluids fractionate Ge isotopes with a range in $\delta^{74}Ge$ between −0.4‰ and −1.4‰ relative to a Columbia River basalt. We cautiously interpret the observed fractionation as preferential removal of heavy Ge isotopes out of solution during cooling of the hydrothermal fluid and subsequent precipitation of quartz.
© 2006 Elsevier Inc. All rights reserved.

## 1. Introduction

As iterated by numerous authors, Ge and Si have similar chemistries in the natural environment (Goldschmidt, 1926, 1958; Froelich and Andreae, 1981; Froelich et al., 1985a,b). As with Si, the typical coordination for inorganic bound Ge is tetrahedral and both dissolved species (silicic and germanic acids) can be present as a tetravalent hydroxide complex (Bernstein, 1985; Pokrovski and Schott, 1998). Therefore, in combination with their similar ionic and covalent radii, it is not surprising that substitution of Ge for Si in mineral phases is common (e.g., Bernstein, 1985; Pokrovski and Schott, 1998).

The close coupling between dissolved germanic and silicic acids throughout the global ocean has been well documented (Froelich and Andreae, 1981; Froelich et al., 1985a,b, 1989; Mortlock and Froelich, 1987). This coupling is demonstrated by their close correlation within the ocean's water column, which exhibits a dissolved Ge:Si ratio of ~0.7 μmol Ge per mol Si. Despite the apparent similarity in their oceanic behaviors, Ge and Si exhibit marked differences in their oceanic sources and sinks. Rivers supply most of the silica to the modern ocean ($5.6 \times 10^{12}$ mol Si $y^{-1}$) with minor contributions from aeolian sources, hydrothermal input, and low-temperature basalt weathering, with these minor sources totaling $\sim 1.4 \times 10^{12}$ mol Si $y^{-1}$ (Treguer et al., 1995; DeMaster, 2002; Wheat and McManus, 2005). The output term for Si is marine biogenic sediments (primarily as diatoms, sponges, and radiolaria) and totals $6.5–7.4 \times 10^{12}$ mol Si $y^{-1}$ (Treguer et al., 1995; DeMaster, 2002). The residence time of Si in the oceans is thought to be less than 20 kyr (e.g., Hammond et al., 2004). In contrast to silica, germanium has two primary sources: rivers, which

* Corresponding author.
E-mail addresses: Christopher.Siebert@asu.edu (C. Siebert), mcmanus@coas.oregonstate.edu (J. McManus).

0016-7037/$ - see front matter © 2006 Elsevier Inc. All rights reserved.
doi:10.1016/j.gca.2006.06.007

contribute $3.3 \times 10^6$ mol Ge $y^{-1}$, and hydrothermal inputs, which contribute 4.9 to $7.1 \times 10^6$ mol Ge $y^{-1}$ (Mortlock et al., 1993; Elderfield and Schultz, 1996; Wheat and McManus, 2005). Aeolian inputs and low-temperature basalt weathering reactions each contribute 0 to $0.4 \times 10^6$ mol Ge $y^{-1}$ to the ocean budget (Mortlock et al., 1993; Elderfield and Schultz, 1996; King et al., 2000). The global ocean sink terms for Ge are biogenic opal, which accounts for $\sim 4.8 \times 10^6$ mol Ge $y^{-1}$, or nearly half of the Ge oceanic input with the balance ($\sim 5.4 \times 10^6$ mol Ge $y^{-1}$) being burial within a non-opaline phase that forms in iron-rich reducing sedimentary environments (Hammond et al., 2000; King et al., 2000; McManus et al., 2003; Wheat and McManus, 2005). The residence time of inorganic Ge in the oceans is <10 kyr (e.g., Hammond et al., 2004).

The differences in the relative importance of the source terms for Ge and Si, combined with the fact that siliceous microfossils may record the water column Ge:Si ratio, has led to the proposal that the Ge:Si ratio recorded in diatoms could serve as a monitor for the relative importance of these two sources through time (e.g., Froelich and Andreae, 1981; Shemesh et al., 1989; Mortlock et al., 1993). The prerequisite for this application as a paleoproxy is that the two elements have sinks that do not discriminate between them, and that biological discrimination between Ge and Si is negligible in the whole ocean. However, the fact that there appears to be a large non-opal sink for Ge (Hammond et al., 2000; King et al., 2000; McManus et al., 2003) coupled with evidence suggesting that there might be at least some biological discrimination between these two constituents (Rubin et al., 2002; Ellwood and Maher, 2003) complicates the interpretation of variations in the oceanic Ge:Si ratio. Our work is motivated by the possibility that Ge isotopes might provide an additional constraint for the Ge cycle that would permit the relative rates of weathering and hydrothermal inputs to be deduced provided that Ge isotopes show distinctive isotope fractionation during a number of the above processes. Toward this end, the goal of this study is twofold: (1) describe a technique for the analysis of Ge isotopes at low sample concentrations and (2) to further establish that Ge isotope fractionation exists in nature. For the present work we examine the Ge isotope composition of high temperature springs located in the Cascade Range of the U.S. Pacific Northwest. With these data we discuss the potential for isotope fractionation under high-temperature conditions, with the caveat that there are difficulties in extrapolating terrestrial systems to the marine environment.

### *1.1. Ge in high temperature systems*

Ge is enriched in both oceanic and terrestrial high-temperature fluids relative to ocean and river waters (e.g., Arnorsson, 1984; Froelich et al., 1985a,b; Criaud and Fouillac, 1986; Mortlock et al., 1993; Evans and Derry, 2002). Concentrations in marine hydrothermal waters are generally in the range of 1–10 nmol $kg^{-1}$ in contrast to river or ocean waters, which contain approximately 0.1–200 pmol Ge $kg^{-1}$. High-T marine hydrothermal fluid Ge:Si ratios vary between 1 and 45 μmol $mol^{-1}$ with a global mean estimated to be ~10 μmol $mol^{-1}$ (Mortlock et al., 1993). In contrast to marine high temperature systems, continental Ge:Si ratios vary considerably from 2 to 1000 μmol $mol^{-1}$ (Arnorsson, 1984; Criaud and Fouillac, 1986; Mortlock and Froelich, 1987; Evans and Derry, 2002; Wheat and McManus, 2005). Modeling suggests that quartz solubility is one control on the Ge:Si ratio in high temperature fluids and that Ge lattice substitution plays an important role (e.g., Evans and Derry, 2002, also see Arnorsson, 1984 and Mortlock et al., 1993). Accordingly data from the Himalaya show some relationship between Si concentrations and Ge:Si ratios (Evans and Derry, 2002). However, any relationship between Ge:Si and another dissolved component or temperature is likely to be influenced by multiple factors. Because of these multiple influences simple relationships are not apparent in the data (e.g., Evans and Derry, 2002). Some of the other processes that may influence the fluid Ge:Si ratio include the precipitation of sulfides and non-equilibrium behavior (e.g., Evans and Derry, 2002). Given the lack of published Ge isotope analysis and theoretical predictions for Ge isotope fractionation, it is at this time difficult to predict how, or if, these various processes may fractionate Ge isotopes.

## 2. Study sites: Geothermal systems in the cascades, Oregon

Cascade Range volcanism is related to the subduction of the Juan de Fuca Plate, and the subduction system has probably been active since the Eocene (45 Ma) (e.g., Sherrod and Smith, 1989). Volcanism decreased in most of the Cascade System at ~17 Ma, but the Oregon Cascade Range has been active for the last 14 Ma (e.g., Sherrod and Smith, 1989). The Cascade Range of central Oregon has a relatively high geothermal potential with one clear expression of this potential being hot spring discharge (e.g., Sherrod and Smith, 1989; Mariner et al., 1990). The source of most of the ground water discharged in these hot springs is the High Cascades (Ingebritsen et al., 1994). Topographically controlled groundwater delivery feeds most of the Western Cascades, where the investigated hot springs discharge at a similar elevation (e.g., Ingebritsen et al., 1994). Approximate temperatures and fluid composition data for the hot springs investigated here are summarized in Table 1, and an extensive literature exists for these springs as noted.

## 3. Double spike Ge isotope analyses: Principles, experimental design, and calibration

### *3.1. Analytical challenges*

Germanium has five stable isotopes (76 (7.44%), 74 (35.94%), 73 (7.73%), 72 (27.66%) and 70 (21.23%)) of

Table 1
Location and previously published background data for the analyzed hot springs, Cascade Range, Oregon

| | McCredie[a] | Paulina Lake[a] | East Lake[a] | Bigelow[b] | Belknap[b] | Terwilliger[b] | Kahneeta[b] |
|---|---|---|---|---|---|---|---|
| *All concentrations in mg/l* | | | | | | | |
| Longitude | 122 17.2W | 121 15W | 121 11.9W | 122 03.30W | 122 02.54W | 122 14.00W | 121 12.00W |
| Latitude | 43 42.2N | 43 43.6N | 43 43.2N | 44 14.21N | 44 11.39N | 44 04.57N | 44 51.42N |
| Elevation (m) | | | | 561 | 493 | 530 | 440 |
| Temp. sampling (°C) | 74 | 52 | 57 | 59 | 73 | 46 | 83 |
| Temp. max. (°C) | | | | 155 | 152 | 135 | 137 |
| pH | 7.3 | 7.3 | 6.1 | 7.8 | 7.6 | 8.5 | 8.1 |
| Na | 1000 | 110 | 56 | 675 | 660 | 405 | 325 |
| K | 21 | 13 | 9.7 | 15 | 15 | 6.1 | 11 |
| Mg | 1 | 42 | 33 | 0.53 | 0.34 | 0.07 | 0.05 |
| Ca | 485 | 50 | 73 | 195 | 210 | 215 | 13 |
| Cl | 2150 | 5 | 1 | 1250 | 1200 | 790 | 155 |
| $SO_4$ | 235 | 2 | 120 | 140 | 150 | 240 | 31 |
| $HCO_3$ | 23 | 689 | 413 | 22 | 20 | 21 | 603 |
| Si ($SiO_2$) | 72 | 184 | 197 | 73 | 91 | 47 | 78 |
| $\delta^{18}O$ | −12.3 | −14.3[c] | −15.1[c] | −11.8 | −11.8 | −12.2 | −14.8 |

[a] Mariner et al. (1990).
[b] Ingebritsen et al. (1994).
[c] Carothers et al. (1987).

which four can be used for isotope analysis (see below). Various efforts to measure the Ge isotope composition of terrestrial and meteoritic samples by Thermal Ionization Mass Spectrometry (TIMS) showed limited success with uncertainties of up to 3‰ (e.g., Green et al., 1986; Richter et al., 1999). This uncertainty is high considering the anticipated small range of terrestrial Ge isotope fractionation in nature. In addition, relatively high amounts of Ge are needed for these measurements. Hirata (1997) showed that Ge isotope measurements with MC-ICP-MS had a potential to increase the precision to <0.3‰. Galy et al. (2003) presented measurements of Ge standard solutions using a desolvating nebulizer system and MC-ICP-MS with an external standard reproducibility that is less than 0.2‰. However, 0.2 μg Ge is required for these measurements, which is a relatively large quantity given that Ge in fluids is a trace constituent having concentrations that are typically five to six orders of magnitude lower than silicon.

### 3.2. Double spike design and calibration

For our approach, we use a $^{73}Ge/^{70}Ge$ double spike to correct for analytical mass fractionation of Ge isotopes and to determine the natural mass dependent fractionation in our sample. This approach has been successfully applied for other heavy stable isotope systems (Ca, Russell et al., 1978; Hippler et al., 2003, Fe, Johnson and Beard, 1999, (TIMS); Mo, Siebert et al., 2001; Fe, Dideriksen et al., 2006; Zn, Bermin et al., 2006, (MC-ICP-MS)) and allows us to correct for mass bias induced during sample preparation or sample introduction. Ge masses 73 and 70 were chosen as spike isotopes, because potential isobaric and molecular interferences can be accounted for and their relative abundances are lower than the measured natural ratio. The Ge isotopes used for spike production were fused from Ge oxide. The composition of the spike was adjusted to a ratio of 1:1 for the spike isotopes $^{73}Ge$ and $^{70}Ge$ (the natural ratio is ~0.38; Table 2), which showed the best mass bias correction performance. Other compositions were tested and the iteration used to determine the instrumental mass bias (e.g., Siebert et al., 2001) did not converge on a single solution resulting in high internal errors during measurements. The sample ratio analyzed and presented in this study is $^{74}Ge/^{72}Ge$. This ratio has a mass difference between the numerator and denominator that is as close as possible to the spike ratio given the distribution of Ge isotopes. Optimizing these ratios allows for more accurate instrumental mass fractionation correction (e.g., Siebert et al., 2001; Vance and Thirlwall, 2002). For analysis we employ a hydride generation system, which converts germanic acid to $GeH_4$ (e.g., Mortlock and Froelich, 1996, also see Hammond et al., 2000 and references therein).

The double spike composition is calibrated relative to a GFS Chemicals, Inc., 1000 ppm Ge ICP standard solution, Lot. Number: L610965. The method for double spike and standard calibration was adopted from Siebert et al. (2001).

Table 2
Results of standard and spike ratio calibrations

| | $^{74}Ge/^{70}Ge$ | 2 SD | $^{73}Ge/^{70}Ge$ | 2 SD | $^{72}Ge/^{70}Ge$ | 2 SD |
|---|---|---|---|---|---|---|
| Standard | 1.770 | $2.8\times10^{-4}$ | 0.3752 | $2.9\times10^{-5}$ | 1.333 | $1.4\times10^{-4}$ |
| Spike | 0.0295 | $2.2\times10^{-5}$ | 0.998 | $4.2\times10^{-4}$ | 0.0278 | $2.8\times10^{-5}$ |

Ge standard and spike solutions were doped with Ga. The $^{73}Ge/^{70}Ge$ ratio of the spike was then measured and the instrumental mass fractionation was corrected using the $^{71}Ga/^{69}Ga$ ratio of 0.663 (Parrington et al., 1996). The same was done for the Ge standard solution. Uncertainties of this "element doping" procedure were kept to a minimum by measuring both standard and spike solutions within the same run parameters during the same day. In addition, and in contrast to sample measurements, no matrix effects are to be expected while measuring pure Ge and Ga solutions. Provided that possible differences in the fractionation behavior of Ga and Ge are constant, the Ge ratios are calibrated relative to each other, which is sufficient for our purposes. The $^{73}Ge/^{70}Ge$ ratio of the spike defined in this way is operationally dependent on the $^{71}Ga/^{69}Ga$ ratio used. Measuring the pure Ge solutions and correcting the ratios for instrumental mass bias with the $^{73}Ge/^{70}Ge$ ratios of the respective solution obtained in the prior step then define all other Ge isotope ratios of the spike and standard solutions. By using this approach all Ge ratios in the spike as well as in the standard used are calibrated relative to each other. To keep mass fractionation and memory effects during spike and standard calibration to a minimum, all calibration measurements were performed using a wet nebulizing introduction system (Micromist low uptake nebulizer (200 μl) and a water cooled cyclonic spray chamber, Glass Expansion, Camberwell, Victoria, Australia). Note that the Ga element doping approach is only used for the initial spike and standard calibration. All subsequent sample measurements are performed using these calibrated ratios.

Various spike and standard mixtures were then measured to test the accuracy of the calibration and the data reduction mathematics. It was found that the spike to sample ratio required for mass fraction correction induced by the hydride generator and mass spectrometer is fairly robust between a ratio of 2 and 6 (Fig. 1), and we chose a spike to sample (in this case $^{70}Ge/^{72}Ge$) ratio of approximately 3–4. Ge concentrations for each sample were determined using a quadrupole ICP-MS prior to sample spiking. For all measurements the spike to sample ratio of spiked standards and samples was kept similar as well as the approximate concentration of the solutions to ensure maximum accuracy of the mass spectrometer mass bias correction. Each sample was analyzed in triplicate using the double spike technique. In addition, a spiked standard was measured before and after every sample run.

Our results are presented in the delta notation relative to the calibrated standard. Using the data reduction technique described in Siebert et al. (2001), a delta value for every single measurement is calculated and the statistics are done on these values. Therefore no extra error propagation is necessary. The standard solution employed here contains Ge as a salt ($(NH_4)_2GeF_6$ in $H_2O$), and although we do not expect there to be substantial isotope fractionation during production, we are aware that the isotope composition of artificial standards can be fractionated from natural compositions during enrichment. At this point in time there is no commonly agreed upon standard for Ge isotopes. Therefore, in addition to the standard solution measured during analyses, we analyzed a number of aliquots from an in-house Columbia River Basalt standard (OSU BCR-3), and an in-house diatom standard. Both of these standards are 0.6‰ lighter than our standard solution (Fig. 2 and discussed below).

### 3.3. Isobaric interferences

Potential isobaric interferences result from $^{76,74}Se$ and $^{70}Zn$. We anticipated that Se would be significantly more problematic than Zn. Zn hydride extraction occurs in an acidic media (Smichowski et al., 2003), whereas the Ge extraction occurs in a near neutral solution. Based on this reasoning and our anticipation that a Zn interference would cause large isotope effects (i.e., large and not reproducible $\delta^{74/72}Ge$ values), we assumed that there was no contribution from a Zn interference. Future work, particularly on Zn-rich samples should consider this possibility, however. In contrast, Se tends to form hydrides similar

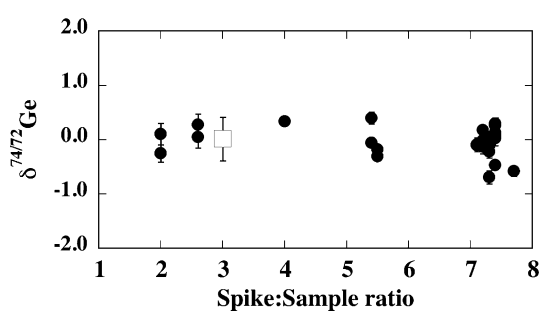


Fig. 1. Measured $\delta^{74/72}Ge$ plotted as a function of the $^{72}Ge/^{70}Ge$ ratio of spiked standards (i.e., an expression of the spike to sample ratio). The $^{72}Ge/^{70}Ge$ ratio of spiked standard measurements was in general kept at 3 (shown as an open square) representing ~60 measurements. The uncertainty given for that value represents the maximum uncertainty for all the measurements made (mean of that value is 0.1‰). Spiked standards with $^{72}Ge/^{70}Ge$ ratios between 2 and 7 can be reproduced within the overall standard reproducibility of 0.4‰ underpinning the robustness of the mass fractionation correction.

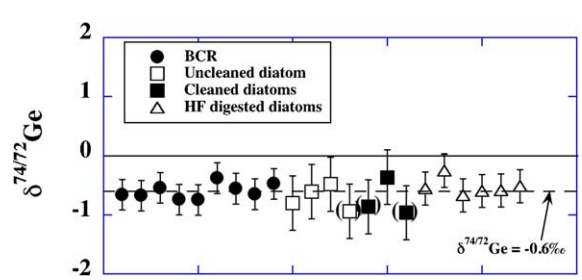


Fig. 2. $\delta^{74/72}Ge$ of basalt standard BCR-3 and the diatom in-house standard. Uncertainties are the 2 SD of the mean for each grouping where the BCR-3 samples (filled circles) form one grouping, the alkaline digested diatoms another (squares), and the HF-digested diatoms the third group (open triangles). The dashed line is −0.6‰, which is the average result for BCR-3. Samples in brackets represent measurements that had low or unstable signals.

to Ge. $^{76}$Se is not at issue for our measurements because we do not use the $^{76}$Ge isotope in our analysis (see below). $^{74}$Se does, however, represent a possible interference, and is 0.89% of the total Se abundance. To exclude the possibility that this isobar is present in our analyses, $^{78}$Se, which is 23.61% of the total Se signal, was measured in all samples. The signal was in all cases not distinguishable from the background noise of about >0.00005 V. The background signal is measured during sample runs and subtracted from every measurement. Therefore, the impact of $^{74}$Se on $^{74}$Ge (35.94%) is analytically not significant. To further test this conclusion, we performed measurements on two Ge standard solutions that were doped with a Se standard solution at a Ge:Se ratio of 1:500. The resulting $\delta^{74}$Ge values ($-0.02‰$ and $-0.06‰ \pm 0.24$) are indistinguishable from our standard measurements leading us to conclude that Se was not contributing to our signal.

Although not an isobaric interference, another possible problem regarding measurement of Ge isotope compositions is the presence of large quantities of Si in the sample matrix, which can precipitate at the pH used during Ge extraction. We therefore doped Ge standard solutions with Si standard solutions (10–20 mM) and did not observe a significant effect on the measured ratios (average of $0.17 \pm 0.25$, $n = 7$).

### 3.4. Molecular interferences

Potential molecular interferences in the Ge mass spectrum result mainly from various Ar molecules or their combination with O. Possible interferences are $^{40}Ar^{16}O_2$, $^{36}Ar^{36}Ar^+$ on mass 72, $^{38}Ar^{36}Ar^+$ on mass 74 and $^{36}Ar^{40}Ar$, $^{38}Ar^{38}Ar^+$ on mass 76. During magnet scans on these respective masses using water and sodium borohydride as "blank" with the constant flow hydride generator used for sample analysis, no detectable signal was seen on masses 72 and 74. Mass 76 however showed a signal significantly higher than background (in the 10 mV range), but as indicated above, $^{76}$Ge is not used for Ge isotope measurements. In addition, spiked standards are also interspersed with sample solutions (i.e., "bracketing standards") to account for any additional interference that might be caused by sample solutions.

## 4. Analytical methods and chemistry for hydride generation

Dissolved silicic acid is measured using standard colorimetric techniques adapted for segmented flow analysis (Gordon et al., 1994). For Ge, the principal chemistry used has been published previously (Mortlock and Froelich, 1996), and our particular approach was detailed in Hammond et al. (2000). The yield for this technique is assumed to be greater than 90% based on secondary hydride extractions, which did not produce significant signal. However, part of the necessity for the double spike pertains to the possibility that this technique is not 100% efficient and the effectiveness of the extraction may vary depending on the sample.

The sample is spiked with a Ge double tracer and allowed to equilibrate overnight. Samples are then buffered with TRIS followed by EDTA. The TRIS to sample ratio is approximately 5% and the EDTA to sample ratio is approximately 1.25%. The sample is then diluted to approximately 20 ml with additional DI water. In contrast to inorganic Ge (germanic acid), methylated Ge species should not be present at significant levels in high-T fluids. This was confirmed during a separate analytical run with Quadrupole ICP-MS, where we measured the Ge concentrations of the samples by a hydride generation single isotope dilution technique (e.g., Hammond et al., 2000). Using this technique the organic Ge peak is resolved from the inorganic Ge peak and no organic Ge was observed in the samples. A note of caution is worth iterating here regarding organic Ge species. Organic species are typically quite important in natural, low temperature environments, and our constant flow hydride generation technique cannot separate these species. For the analysis of fluid samples containing high amounts of organic Ge chemical separation prior to measurements would be required.

For measurements, inorganic Ge is converted to germane ($GeH_4$) in a reaction coil using approximately 4% sodium borohydride and He as a carrier gas. In contrast to techniques for Ge concentration measurements published earlier, the measurement of Ge isotopes with a MC-ICP-MS requires relatively long measurement duration with a relatively stable signal. These criteria are achieved using a constant flow hydride generator (Fig. 3), modified after Rouxel et al. (2002). The sample solution reacts with the sodium borohydride in an approximately 40 cm long HDPE mixing coil followed by an approximately 30 cm long glass mixing coil. Helium is injected as a carrier gas at the beginning of the mixing coils. The sample uptake occurs via a peristaltic pump and pumping ratios are about 1 ml per minute of sodium borohydride into approximately 10 ml per min. of sample solution. As the solution drips into a gas liquid separator the volatile $GeH_4$ is stripped from solution by additional He carrier gas induced through a frit at the bottom of the gas/liquid separator. Helium gas flow for both injections is $0.6\ l\ min^{-1}$. From the gas liquid separator the gas is carried over a moisture trap (Mg-perchlorate) and an additional $CO_2$ trap. The sample gas is then mixed with Ar-gas prior to injection in the ICP plasma.

Each spiked sample is corrected for mass fractionation during data reduction (e.g., Siebert et al., 2001). Spiked standards are measured and treated as unknown samples between each sample run to account for any drift during analyses. The average standard value for each measurement session is then subtracted from the corrected samples to assure that results are comparable with previous measurements. In this way, we account for non-reproducible changes in the mass spectrometer and non-reproducible conditions associated with the sample introduction system. The measured standards on the hydride generation system are thus always compared to the standard calibrated on a

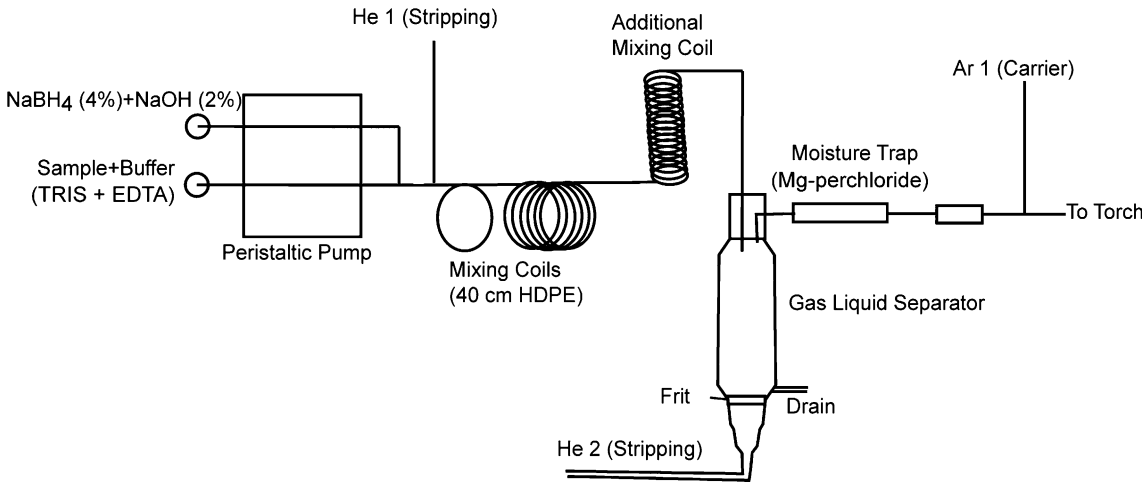


Fig. 3. Schematic of the constant flow hydride generator used for this study (modified after Rouxel et al., 2002).

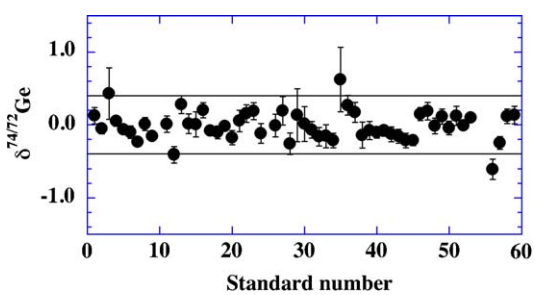


Fig. 4. Reproducibility of spiked standards measured by hydride generation and double spike technique over several measurement sessions. Solid lines represent ±0.4‰, which brackets all but 3 of our standard measurements out of 52 total measurements. We give a conservative estimation of 0.4‰ as the overall reproducibility of our method.

"normal" nebulizer and cyclonic spraychamber, which are assumed to have considerably less fractionation.

Results of standard measurements for several measurement sessions are shown in Fig. 4. Individual measurement days show the day to day reproducibility of spiked standards is between 0.14‰ and 0.32‰ $\delta^{74/72}$Ge (2 SD). The average standard reproducibility is 0.4 ‰ (2 SD) over a period of several months (Fig. 4). Internal errors are typically ~0.2‰ (2 SE) or better.

## 5. Mass spectrometry

Isotope measurements are made on a Nu Instruments HR MC-ICP-MS (Wrexham, North Wales, UK) in the W.M. Keck Collaboratory at Oregon State University. An electrostatic analyzer is used to focus the ion beam with high energy dispersion and two electrostatic lenses behind the magnet allow for varied dispersion of the ion beam into a static collector array of 12 Faraday cups.

Typical analyte consists of about 20 ml of sample solution with minimum Ge concentrations of 100 ppt (2 ng total Ge) resulting in a typical total signal of 1.5–2 V. Signals or measurement time lower than that did result in increased internal errors and decreasing reproducibility. An increase in signal strength or measurement time or both will increase measurement statistics and presumably lower errors. Internal errors (~±0.2‰) are generally smaller than external errors (~±0.4‰). Measurements make use of 4 of the 12 Faraday cups (H4, H2, Ax and L2) and masses 74, 73, 72 and 70 are measured simultaneously in static mode. Each measurement cycle is integrated for 10 s and a total of 20 cycles (2 blocks) are measured during one run. All sample data presented here consist of 3 runs with the exception of one sample where the initial run was erratic, meaning that we could not establish a stable signal (Table 3).

Scans of the Ge mass spectrum did not show signals for Se, Zn or other interferences when aspirating blank solution (on-peak-zero). Therefore, background is measured before every block for 15 s by deflecting the Electrostatic Analyzer (ESA) of the instrument. Background reproducibility is 0.01 mV for a 10 s integration. Because memory effects can produce systematic errors using a double spike, the hydride generator system was washed out with water until the normal background signal of >0.00005 V was stable between measurements.

## 6. Mass bias correction

Natural and instrumental mass dependent isotope fractionation is assumed to follow the exponential law. This assumption has proven the most accurate in a variety of isotope studies, despite the fact that the law might not correct perfectly for mass discrimination on every mass spectrometer (e.g., Rehkämper and Halliday, 1998; Marechal et al., 1999; Vance and Thirlwall, 2002; Archer and Vance, 2004). The three dimensional data reduction procedure is adopted from Siebert et al. (2001) and is based on prior work (Hofmann, 1971; Russell et al., 1978, and Johnson and Beard, 1999). The data reduction follows the mathematics described in Siebert et al. (2001). This data reduction procedure results in a delta value for every single

Table 3
Results for Ge isotope measurements of Cascade hot spring samples

| | Paulina Lake $\delta^{74/72}$Ge | Bigelow $\delta^{74/72}$Ge | Terrwiliger $\delta^{74/72}$Ge | East Lake $\delta^{74/72}$Ge | McCredie $\delta^{74/72}$Ge | Kahneeta $\delta^{74/72}$Ge |
|---|---|---|---|---|---|---|
| 1 | −1.4 | −1.7 | | −1.0 | −1.9 | −1.5 |
| 2 | −1.3 | −2.2 | −1.6 | −1.2 | −1.4 | −1.4 |
| 3 | −1.2 | −2.0 | −1.8 | −1.0 | −1.7 | −1.7 |
| Ave./Std[a] | −1.3 | −2.0 | −1.7 | −1.0 | −1.7 | −1.5 |
| SD | 0.1 | 0.3 | 0.1 | 0.1 | 0.2 | 0.1 |
| Ave./BCR[b] | −0.7 | −1.4 | −1.1 | −0.4 | −1.1 | −0.9 |
| SD | 0.3 | 0.4 | 0.3 | 0.3 | 0.4 | 0.3 |

[a] Ave./Std. is the isotope value relative to our laboratory standard.
[b] Ave./BCR. is the isotope value relative to our BCR laboratory standard. Uncertainties are 1 $\sigma$ of the mean and in the case of the BCR, uncertainties in both the BCR and the mean value are propagated.

cycle measured, so that no error propagation is needed for the resulting mean delta value of each run. In addition to the Ge isotope composition, precise Ge concentrations are determined with each run via the measured spike to sample ratio.

## 7. Results and discussion

### 7.1. Basalt and diatom samples

Although there is no accepted standard, we reference our results to both our liquid standard as well as an in-house basalt standard (e.g., Table 3). For dissolution of the basalt sample we followed standard rock digestions techniques (e.g., Siebert et al., 2001). This technique is a standard HF, $HNO_3$ digestion with the modification of having added double spike to the sample before digestion. We were concerned that this rock dissolution technique, which uses HF could volatilize Ge similar to Si, thus we also performed a set of experiments where we digested a set of diatom samples (a nearly pure Si matrix) using both an alkaline digestion and an HF digestion (e.g., Fig. 2).

Our in-house diatom standard has an unknown history. However, based on our work here as well as other work in our laboratory, the sample appears homogeneous and was cleaned of contaminant phases. In digesting and analyzing this sample for its Ge:Si ratio it was found to have a Ge:Si ratio of $0.38 \pm 0.02$ (μmol mol$^{-1}$) with there being no difference between diatoms that underwent further cleaning and those that did not. For additional cleaning and diatom dissolution we followed the protocol of Shemesh et al. (1988) and for alkaline digestion we use 2 M NaOH. Samples show no resolvable difference in Ge isotope compositions between the different cleaning and digestion techniques. The diatoms that were digested using the alkaline technique have greater scatter, but these results are indistinguishable from the mean for all the data (Fig. 2). One of the more striking results from these experiments is the nearly uniform value of both BCR-3 and the diatom standard, ∼−0.6‰ relative to our liquid standard.

### 7.2. High temperature fluid samples

High-T hydrothermal fluids from a number of locations in Oregon (Table 1) were analyzed for Ge isotope composition, Ge concentrations and Si concentrations (Tables 3 and 4). Ge:Si ratios range from 6 to 74 μmol mol$^{-1}$ (Table 4), and all samples show light Ge isotope compositions ranging from $\delta^{74/72}$Ge = −1‰ to −2‰ relative to the analytical standard and $\delta^{74/72}$Ge = −0.4 to −1.4‰ relative to the Basalt Standard BCR-3 (Fig. 5 and Table 3). For presentation of the isotope data, we separate the two samples that were taken from springs located within Paulina and East Lakes (Fig. 5) from the other spring samples. Although these samples are certainly heavily influenced by geothermal springs, they also are in communication with the open lake. Thus, they might have somewhat different chemistry from the other samples. Consistent with this idea the Ge:Si ratio is significantly different between these two groups (Table 4). This separation also distinguishes the two lake samples from the other spring samples in terms of isotope composition, yielding an average spring value of $-1.1 \pm 0.4$‰ (2 SD), whereas the lake samples are $-0.6 \pm 0.4$‰ (2 SD). However, despite this difference, these numbers at $2\sigma$ are indistinguishable.

The measured Ge:Si ratios (μmol mol$^{-1}$) are higher than those from typical low-temperature weathered fluids (∼<1) and those of bedrock (∼3 or lower) and are more elevated

Table 4
Results for Ge and Si concentrations by ICP-MS

| | Si[a] (μM) | [b]Si (μM) | Ge (μM) | Ge/Si (μmol mol$^{-1}$) |
|---|---|---|---|---|
| McCredie | 1277 | 1077 | 0.094 | 74 |
| Paulina Lake | 3110 | 2752 | 0.020 | 6 |
| East Lake | 3466 | 2947 | 0.026 | 7 |
| Bigelow | 1227 | 1092 | 0.077 | 62 |
| Belknap | 1596 | 1361 | 0.080 | 50 |
| Terwilliger | 783 | 703 | 0.026 | 33 |
| Kahneeta | 1105 | 1167 | 0.071 | 64 |

[a] Results from this study.
[b] Results from prior work, summarized in Table 2.

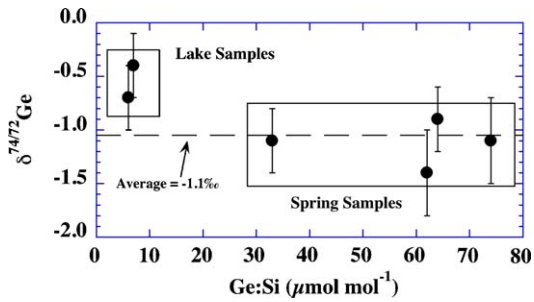


Fig. 5. $\delta^{74/72}$Ge results (relative to BCR-3) of high-T hydrothermal samples versus the Ge:Si ratio. Lake samples show lower Ge:Si ratios and Ge isotope fractionation in comparison to the fluids from hot springs. This might indicate a "dilution" of the original hydrothermal signal in the lake samples by meteoric water. Our hypothesis is that the overall light Ge isotope composition of these fluids (relative to basalt) could be caused by precipitation of quartz during fluid transport fractionating heavy Ge isotopes in the solid (see text).

than Ge:Si ratios known from ocean floor and ridge flank hydothermal systems (<45, e.g., Mortlock et al., 1993; Wheat and McManus, 2005). The ratios are however consistent with the range in Ge:Si ratios observed for continental geothermal systems (e.g., Evans and Derry, 2002 and references therein).

In general, it has been argued that the two most likely processes that explain the high Ge:Si ratios observed in high temperature fluids are (1) an equilibrium reaction between a Ge bearing mineral phase and fluid in the bedrock, and (2) precipitation of a Ge-poor mineral phase (e.g., quartz) during transport and cooling of hydrothermal fluid (e.g., Evans and Derry, 2002). Mortlock et al. (1993) found the highest ratios in fluids with relatively low temperatures and increasing Ge/Si ratios with decreasing Si concentrations in hydrothermal systems in the Pacific Ocean, and this relationship is observed at the sites we sampled (Fig. 6). Precipitation of a Ge-poor phase can explain the increasing Ge:Si ratios and it also might explain the light Ge isotope ratios with respect to basaltic rocks through which these fluids mostly circulate. For example, Evans and Derry (2002) showed that precipitation of quartz (Rayleigh distillation process) could explain the high Ge:Si ratios (up to 1000) in Himalayan hydrothermal fluids with temperatures ranging from 20 to 70 °C. A similar process might occur in the hydrothermal systems of the Cascades where Ge and Si are most likely leached out of the basaltic to andesitic bedrock. Si could then be subsequently depleted by progressive precipitation of quartz during fluid transport from the central to the western Cascades. As observed in our samples (Fig. 6) Si loss from the system could be the main determining factor for the changing Ge:Si ratio.

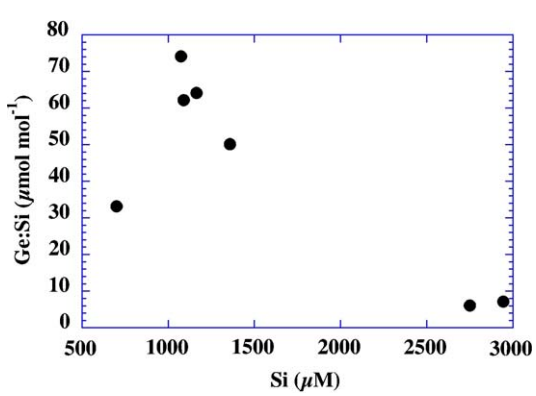


Fig. 6. Plot of Ge:Si ratios versus Si shows decreasing Si contents with decreasing Ge:Si ratios, supporting the idea of Si precipitation as the driving factor for the change in Ge:Si ratios.

We might expect a relationship between the Ge isotope signature and fluid Ge:Si ratios if isotope fractionation is being caused by the loss of Si from the fluid. Essentially, we might expect isotope fractionation to be caused by the preferential removal of heavy Ge isotopes in a precipitating mineral phase (i.e., quartz). However, the analytical uncertainties in our data preclude identifying any relationship between the isotope and the Ge and Si data, and because of the paucity of data on Ge isotope compositions of terrestrial materials any further discussion would be premature. However, it is important to recognize that there are other phases or processes (e.g., Bernstein, 1985; Evans and Derry, 2002) that could be influencing the fluid isotope composition. Whatever the exact mechanism of Ge isotope fractionation during geothermal fluid transport, the fact that the isotopes show fractionation during these processes opens the possibility for the use of Ge isotopes as an additional constraint for the use of Ge:Si ratios as oceanic tracer.

### *7.3. Implications for the Ge/Si ratio as a proxy for ocean chemistry*

Because Ge has two dominant sources (rivers and hydrothermal activity) and two sedimentary sinks (opal and iron-rich sediments) an additional constrain is needed to continue to develop Ge as a useful tracer for the cycling of silicon in the environment. Germanium isotopes offer such a constraint in that it appears that at least during high temperature processes Ge isotopes undergo fractionation. Although tempting, it is not tenable to extrapolate these results to marine hydrothermal systems at this particular time, nor is that our intention here. Rather, the data here point to resolvable isotope fractionation during high temperature water rock interaction, which implies that further exploration of Ge isotope variations is warranted. Oceanic hydrothermal fractionation could be quite different from our results for any one of a number of reasons, but it is important to keep in mind that the marine Ge budget is actually dominated by organic species and the isotopic composition of that organic Ge and its fate during hydrothermal fluid circulation are unconstrained, for example. Furthermore, we reiterate here that in terrestrial high temperature fluids the Ge:Si ratio is quite different (elevated) than in the marine environment (references as above), and that the range in terrestrial Ge:Si dissolved ratios is more than an order of magnitude larger than for marine systems.

Therefore, those processes leading to matrix discrimination of Ge over Si could differ between terrestrial and marine systems. However, if distinctive Ge isotope fractionations are associated with the different Ge reservoirs, Ge isotopes could be the key to understanding the paired Ge–Si system, and Ge isotopes in combination with Ge:Si ratios could evolve into a powerful tool to quantify changes in weathering rates and hydrothermal input to the oceans.

## 8. Conclusions

The combination of MC-ICP-MS, hydride generation as a Ge extraction method, and the double spike approach allows reproducible measurements of the Ge isotope composition of solutions with total Ge concentrations of 2 ng. Differences in sample isotope composition and reference material can be resolved to ±0.4‰. For future work this value could be reduced by improvements to the hydride extraction (i.e., improving the stability of the signal). Possible interferences can be monitored and fractionation during the analytical procedures can be corrected with the described method. However, samples containing organic Ge species (such as seawater) cannot be analyzed with constant flow hydride generation as these species would have to be separated prior to analysis.

Terrestrial hydrothermal water samples show Ge isotope fractionation with values ranging between −0.4‰ and −1.4‰ relative to a basalt sample. Although we yet do not know the fractionation mechanism it is possible that it may be caused by the preferential removal of Si out of solution and the subsequent precipitation of quartz, a low Ge mineral that might prefer the heavier Ge isotopes. Our preliminary study suggests that significant Ge isotope fractionation exists in nature, and if these observations can be verified and expanded, Ge isotopes may offer an additional constraint on using Ge as a tracer for the global silicon cycle.

## Acknowledgments

J.M. extends his sincere gratitude to long time collaborator Doug Hammond, for his many fruitful discussions regarding Ge geochemistry. We thank Bronwen Cumberland and Benjamin McManus for assistance in the field. Andy Ungerer provided tireless assistance and creativity in the laboratory and we thank all associated with the W.M. Keck Collaboratory, and in particular Gary Klinkhammer, for their willingness to contribute to the uncommon vision of a shared analytical facility. We also extend our gratitude to Derek Vance, three anonymous reviewers and the Associate Editor Juske Horita for their constructive criticism. The senior author was supported in part by Swiss NSF Grant PBBE2-102997 and ACS PRF# 40264-AC2. This work was also supported by NSF Grants 0327016 and 0326574 to McManus.

*Associate editor:* Juske Horita

## References

Archer, C., Vance, D., 2004. Mass discrimination correction in multi-collector plasma source mass spectrometry: an example using Cu and Zn isotopes. *J. Anal. Atomic Spectrom.* **19**, 656–665.

Arnorsson, S., 1984. Germanium in Icelandic geothermal systems. *Geochim. Cosmochim. Acta* **48**, 2489–2502.

Bermin, J., Vance, D., Archer, C., Statham, P.J., 2006. The determination of the isotopic composition of Cu and Zn in seawater. *Chem. Geol.* **226** (3-4), 280–297.

Bernstein, L.R., 1985. Germanium geochemistry and mineralogy. *Geochim. Cosmochim. Acta* **49**, 2409–2422.

Carothers, W.W., Mariner, R.H., Keith, T.E.C., 1987. Isotope geochemistry of minerals and fluids from Newberry Volcano, Oregon. *J. Volcanol. Geotherm. Res.* **31**, 47–63.

Criaud, A., Fouillac, C., 1986. Etude des eaux thermominérales carbogazeuses du Massif Central Français. II. Comportement de quelques métaux en trace, de l'arsenic de l'antomoine et du germanium. *Geochim. Cosmochim. Acta* **50**, 1573–1582.

DeMaster, D.J., 2002. The accumulation and cycling of biogenic silica in the Southern Ocean: revisiting the marine silica budget. *Deep Sea Res. II* **49**, 3155–3167.

Dideriksen, K., Baker, J.A., Stipp, S.L.S., 2006. Iron isotopes in natural carbonate minerals determined by MC-ICP-MS with a Fe-58–Fe-54 double spike. *Geochim. Cosmochim. Acta* **70** (1), 118–132.

Elderfield, H., Schultz, A., 1996. Mid-ocean ridge hydrothermal fluxes and the chemical composition of the ocean. *Ann. Rev. of Earth Planet. Sci.* **24**, 191–224.

Ellwood, M.J., Maher, W.A., 2003. Germanium cycling in the waters across a frontal zone: the Chatam Rise. *N Z Mar. Chem.* **80**, 145–159.

Evans, M.J., Derry, L.A., 2002. Quartz control of high germanium/silicon ratios in geothermal waters. *Geology* **30** (11), 1019–1022.

Froelich, P.N., Kaul, L.W., Bird, J.T., Andreae, M.O., Roe, K.K., 1985b. Arsenic, barium, germanium, tin, dimethylsulfide and nutrient biogeochemistry in Charlotte Harbor, Florida, a phosphorus-enriched estuary. *Estuarine Coastal Shelf Sci.* **20**, 239–264.

Froelich, P.N., Mortlock, R.A., Shemesh, A., 1989. Inorganic germanium and silica in the Indian Ocean: biological fractionation during Ge/Si opal formation. *Global Biogeochem. Cycles* **3**, 79–88.

Froelich, P.N., Andreae, M.O., 1981. The marine geochemistry of germanium: Ekasilicon. *Science* **213**, 205–207.

Froelich, P.N., Hambrick, G.A., Andrae, M.O., Mortlock, R.A., 1985a. The geochemistry of inorganic germanium in natural waters. *J. Geophys. Res.* **90**, 1133–1141.

Galy, A., Pomies, C., Day, J.A., Pokrovsky, O.S., Schott, J., 2003. High precision measurement of germanium isotope ratio variations by multiple collector-inductively coupled mass spectrometry. *J. Anal. Atomic Spectrom.* **18**, 115–119.

Goldschmidt, V.M., 1926. Uber das krystallochemisches und geochemisches Verhalten des Germaniums. *Naturwissenshaften* **14**, 295–297.

Goldschmidt, V.M., 1958. *Geochemistry*. Oxford University Press, Oxford.

Gordon, L.I., Jennings, J. C., Ross, A.A., Krest, J.M., 1994. A suggested protocol for continuous flow automated analysis of seawater nutrients (phosphate, nitrate, nitrite and silicic acid) in the WOCE Hydrographic Program and the Joint Global Ocean Fluxes Study. WOCE Operations Manual, vol. 3: The Observational Programme Section 3.1: WOCE Hydrographic Programme, Part 3.1.3: WHP Operations and Methods (WHP Office Report WHPO 91-1; WOCE Report No. 68/91), Revision 1, Woods Hole, Mass., USA, Loose-leaf, p. 52

Green, M.D., Rosman, K.J.R., de Laeter, J.R., 1986. The isotopic composition of germanium in terrestrial samples. *Int. J. Mass Spectrom. Ion Process.* **68** (1–2), 15–24.

Hammond, D.E., McManus, J., Berelson, W.M., Meredith, C., Klinkhammer, G.P., Coale, K.H., 2000. Diagenetic fractionation of Ge and Si in reducing sediments: the missing Ge sink and a possible mechanism to cause glacial/interglacial variations in oceanic Ge/Si. *Geochim. Cosmochim. Acta* **64**, 2453–2465.

Hammond, D.E., McManus, J., Berelson, W.M., 2004. Oceanic germanium:silicon ratios: evaluation of the potential overprint of temperature on weathering signals. *Paleoceanography* **19**, PA2016. doi:10.1029/2003PA00094.

Hippler, D., Schmitt, A.D., Gussone, N., Heuser, A., Stille, P., Eisenhauer, A., Nägler, T.F., 2003. Calcium isotopic composition of various reference materials and seawater. *Geostandards Newsletter* **27** (1), 13–19.

Hirata, T., 1997. Isotopic variations of germanium in iron and stony meteorites. *Geochim. Cosmochim. Acta* **61** (20), 4439–4448.

Hofmann, A., 1971. Fractionation corrections for mixed-isotope spikes of Sr, K, and Pb. *EPSL* **10**, 397–402.

Ingebritsen, S.E., Mariner, R.H., Sherrod, D.R., 1994. Hydrothermal systems of the cascade range, North-Central Oregon. In: Geohydrology of geothermal systems (Ed. U. S. G. S. p. paper). U.S. Department of the Interior, U.S. Geological Survey.

Johnson, C.M., Beard, B.L., 1999. Correction of instrumentally produced mass fractionation during isotopic analysis of Fe by thermal ionisation mass spectrometry. *Int. J. Mass Spectrom.* **193**, 87–99.

King, S.L., Froelich, P.N., Janhke, R.A., 2000. Early diagenesis of germanium in sediments of the Antarctic South Atlantic: in search of the missing Ge sink. *Geochim. Cosmochim. Acta* **64**, 1375–1390.

Marechal, C.N., Telouk, P., Albarede, F., 1999. Precise analysis of copper and zinc isotopic compositions by plasma-source mass spectrometry. *Chem. Geol.* **156**, 251–273.

Mariner, R.H., Presser, T.S., Evans, W.C., Pringle, M.K.W., 1990. Discharge rates of fluid and heat by thermal springs of the cascade range, Washington, Oregon, and Northern California. *J. Geophys. Res.* **96** (B12), 19,517–19,531.

McManus, J., Hammond, D.E., Cummins, K., Klinkhammer, G.P., Berelson, W.M., 2003. Diagenetic Ge–Si fractionation in continental margin environments: further evidence for a non-opal Ge sink. *Geochim. Cosmochim. Acta* **67**, 4545–4557.

Mortlock, R.A., Froelich, P.N., Feely, R.A., Massoth, G.J., Butterfield, D.A., Lupton, J.E., 1993. Silica and germanium in Pacific Ocean hydrothermal vents and plumes. *Earth Planet. Sci. Lett.* **119**, 365–378.

Mortlock, R.A., Froelich, P.N., 1987. Continental weathering of germanium: Ge/Si in the global river discharge. *Geochim. Cosmochim. Acta* **51**, 2075–2082.

Mortlock, R.A., Froelich, P.N., 1996. Determination of germanium by isotope dilution-hydride generation inductively coupled plasma mass spectrometry. *Anal. Chimica Acta* **322**, 5638–5645.

Parrington, J.R., Knox, H.D., Breneman, S.L., Baum, E.M., Feiner, F., 1996. Nuclides and Isotopes, Chart of the Nuclides. GE Nuclear Energy.

Pokrovski, G.S., Schott, J., 1998. Thermodynamic properties of aqueous Ge(IV) hydroxide complexes form 25 to 350°: implications for the behavior of germanium and the Ge/Si ratio in hydrothermal fluids. *Geochim. Cosmochim. Acta* **62**, 1631–1641.

Rehkämper, M., Halliday, A.N., 1998. Accuracy and long-term reproducibility of lead isotopic measurements by multiple-collector inductively coupled plasma mass spectrometry using an external method for correction of mass discrimination. *Int. J. Mass Spectrom.* **181** (1-3), 123–133.

Richter, F.M., Liang, Y., Davis, A.M., 1999. Isotope fractionation by diffusion in molten oxides. *Geochim. Cosmochim. Acta* **63** (18), 2853.

Rouxel, O., Ludden, J., Carignan, J., Marin, L., Fouquet, Y., 2002. Natural variations of Se isotopic composition determined by hydride generation multiple collector inductively coupled plasma mass spectrometry. *Geochim. Cosmochim. Acta* **66** (18), 3191–3199.

Rubin, S.I., Partin, J.W. Froelich, P.N., 2002. Biological fractionation of Ge/Si by Antarctic diatoms—JGOFS/AESOPS trap results. *Eos Trans.* AGU, 83(47) Fall Meet. Suppl., Abstract PP51A-0290.

Russell, W.A., Papanastassiou, D.A., Tombrello, T.A., 1978. Ca isotope fractionation on the Earth and other solar system materials. *Geochem. Cosmochem. Acta* **42**, 1075–1090.

Shemesh, A.R., Mortlock, R.A., Smith, R.J., Froelich, P.N., 1988. Determination of Ge/Si in marine siliceous microfossils: separation, cleaning, and dissolution of diatoms and Radiolaria. *Mar. Chem.* **25**, 305–323.

Shemesh, A., Mortlock, R.A., Froelich, P.N., 1989. Late Cenozoic Ge/Si record of marine biogenic opal: implications for variations of riverine fluxes to the ocean. *Paleoceanography* **4**, 221–234.

Sherrod, D.R., Smith, J.G., 1989. Preliminary map of upper Eocene to Holocene volcanic and related rocks of the Cascade Range, Oregon. U.S. Geological Survey Open-File Report 89-14, scale 1:500,000.

Siebert, C., Nägler, T. F., Kramers, J.D., 2001. Determination of molybdenum isotope fractionation by double-spike multicollector inductively coupled plasma mass spectrometry. *Geochem. Geophys. Geosyst.* 2, paper number 2000GC000124.

Smichowski, P., Farias, S., Perez Arisnabarreta, S., 2003. Chemical vapour generation of transition metal volatile species for analytical purposes: determination of Zn by inductively coupled plasma-optical emission spectrometry. *Analyst* **128**, 779–785.

Treguer, P., Nelson, D.M., Van Bennekom, A.J., DeMaster, D.J., leynaert, A., Queguiner, B., 1995. The silica balance in the world ocean: a reestimate. *Science* **268**, 375–379.

Vance, D., Thirlwall, M., 2002. An assessment of mass discrimination in MC-ICP-MS using Nd isotopes. *Chem. Geol.* **185**, 227–240.

Wheat, C.G., McManus, J., 2005. The role of ridge-flank hydrothermal systems on the oceanic germanium and silicon balances. *Geochim. Cosmochim. Acta* **69**, 2021–2029.